

Temporal variation of the earth's magnetic field

Bachelor-Arbeit

zur Erlangung des Grades

Bachelor of Science (B.Sc.)

im Studiengang Physik

am Department Physik der
Friedrich-Alexander-Universität Erlangen-Nürnberg

vorgelegt am 15.11.2022

von **Nina Grabmann**

Betreuer: Prof. Dr. Jörn Wilms

Summary

The earth's magnetic field not only makes life on earth possible, but also gives us a lot of information about the earth's structure, particle movements in the atmosphere and solar activity. This thesis focuses on the temporal variation of the earth's magnetic field and I describe the construction and verification of a Raspberry PI based magnetometer. Thereby I find drifts in the measurement results, which are not found in the comparison data. The data show a well known 24 h periodicity caused by current systems in the ionosphere and a 9 min periodicity whose origin is unclear.

Contents

Summary	1
1 The earth's magnetic field	3
2 Three-axis magnetometer	5
2.1 Raspberry PI 4	5
2.2 Analog Digital Converter	5
2.3 Magnetic field sensor FLC100	7
2.4 Temperature sensor TMP102	8
2.5 Wiring diagram	10
3 Analysis software	11
4 Measurements	11
4.1 First three weeks measurement	12
4.1.1 Temperature	12
4.1.2 Magnetic field values in the three dimensions	13
4.1.3 Total magnetic field values	14
4.2 Second four weeks measurement	16
4.2.1 Temperature	16
4.2.2 Magnetic field values in the three dimensions	16
4.2.3 Total magnetic field values	17
5 Temporal variation of the magnetic field	17
5.1 General in/decreases	19
5.2 9.29 min periodicity	20
5.3 24 h periodicity	22
6 Conclusions	24
References	26
Appendix	27
Acknowledgements	31

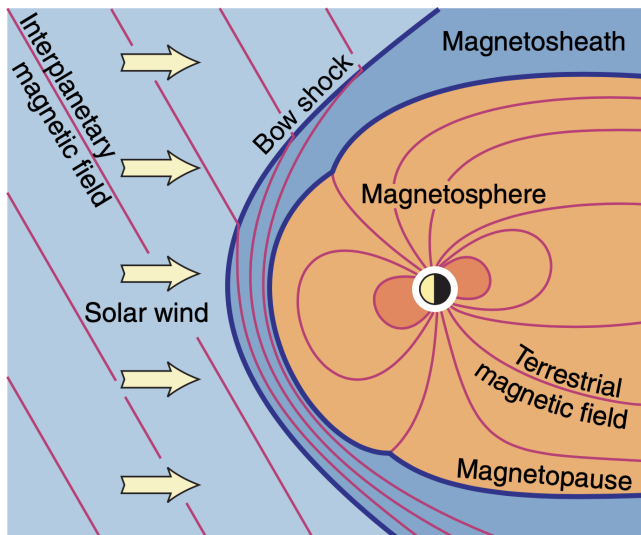


Figure 1: Interaction of the solar wind and earth's magnetic field; (image taken from Schubert, 2007, their Fig. 1 in chapter 3).

1 The earth's magnetic field

The sun constantly sends radiation and charged particles into space, but the areas of high magnetic field strength in the chromosphere can also be a starting point for solar flares (Reda et al., 2022). Usually the magnetic field lines there are closed in arcs. It may happen that the field lines break open and a plasma cloud eruptively escapes into space. Then an x-ray flash occurs (Owocki, 2022) and high-energy particles (mainly protons at about 20 percent of the speed of light) (Matsumoto & Miyoshi, 2022) and the coronal mass ejection (electrons, protons and atomic nuclei at speeds of about 1000 km s^{-1}) are thrown into space (Ponti et al., 2022). These three components can hit the earth's magnetic field, when the direction of the eruption points earthwards.

The terrestrial magnetic field (see Fig. 1) is defined as the magnetic field produced by all sources within and outside the solid earth up to the magnetopause (Schubert, 2007). Sources of this field are mainly two categories. One is magnetized media, which are found inside the solid earth and occur in form of rocks. They were permanently magnetized a long time ago and also show induced magnetization. The other source of the earth's magnetic field are electromagnetic currents (see Fig. 2), which are found inside the earth (metal core, mantle and crust), as well as in the ionosphere and magnetosphere (Schubert, 2007).

When particles from the sun hit the earth's atmosphere, they first enter the ionosphere (50 km to 2000 km), which is divided into D, E, and F layers (Loi et al., 2015). The F layer is between 140 km and 400 km and has the highest electron density. During the day, it is also divided into F1 and F2. F2 is more crucial for the interaction with solar particles and has the higher electron density. The E layer lies between 90 km and 140 km and interacts with lower frequencies than the E layer. Both layers are much stronger during the day than at night (Loi et al., 2015). Between 50 km and 90 km the D layer forms additionally during the day. All are dependent on the time of day and contribute to the deflection of charged particles and thus also to the change of the magnetic field (Dmitriev et al., 2013).

Ionized particles at high energy levels can not only affect the magnetic field as shown in Fig. 1, but also disrupt and destroy technology (Beggan & Marple, 2016). In a digitised and globalized world, this can lead to communication breakdowns, delivery problems and major social crises. Therefore it is important to understand what happens to these particles and

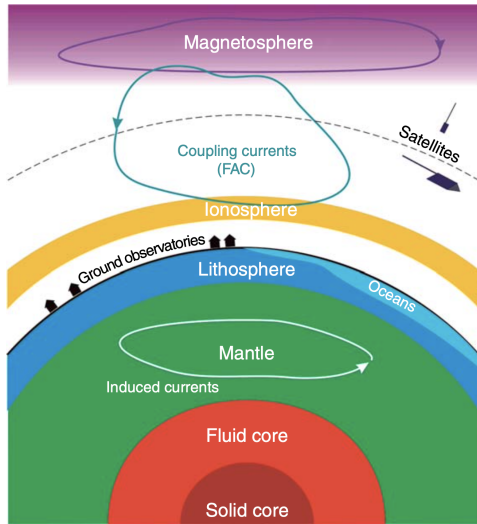


Figure 2: Structure of the earth with the different layers and the currents that contribute to the magnetic field; (image taken from Schubert, 2007, their Fig. 1 in chapter 2).

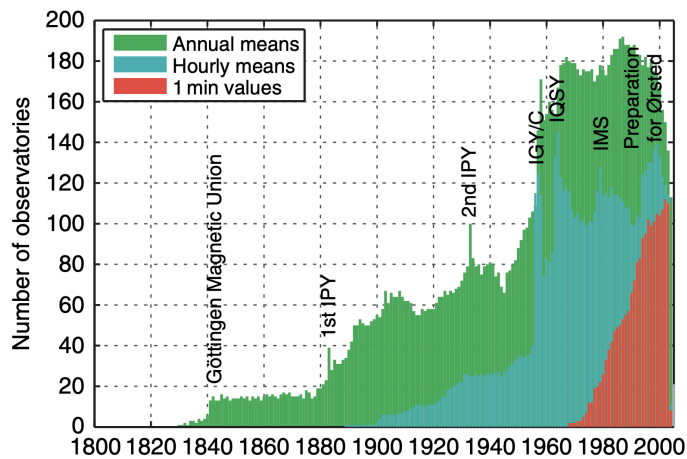


Figure 3: Number of geomagnetic observatories providing annual means, hourly means and 1 min values of magnetic field data, as a function of time; (image taken from Schubert, 2007, their Fig. 6 in chapter 2).

x-rays when they hit the earth's atmosphere.

In research, the number of observatories recording magnetic data is increasing. Historically, the data were given as averaged daily values and were later also measured hourly and minutely (Schubert, 2007). The increase over the years from 1800 to 2000 are shown in Fig. 3.

To study the effects of the solar winds on earth, the terrestrial magnetic field and its daily variations are analyzed in this thesis. This is done with a self-built magnetic field measurement system, including a Raspberry Pi computer according to the paper *Space weather goes to schools* by Beggan & Marple (2016). It is inexpensive and can be replicated at other universities for teaching purposes.

This thesis is structured as follows. In section 2 I talk about the structure of a three-axis magnetometer, which consists of a Raspberry Pi, an Analog Digital Converter, a temperature sensor and three magnetic field sensors. All components are connected and tested. Section 2 ends with a subsection about the wiring diagram. The used analysis software is discussed in section 3. In section 4.1 and 4.2 I talk about the results of two magnetic field measurements that were done at the Dr. Karl Remeis-Observatory in Bamberg. In section 5 the trends, the 9 min and the 24 h periods found in the data are discussed. Suggestions for an improvement of the project are given in section 6.

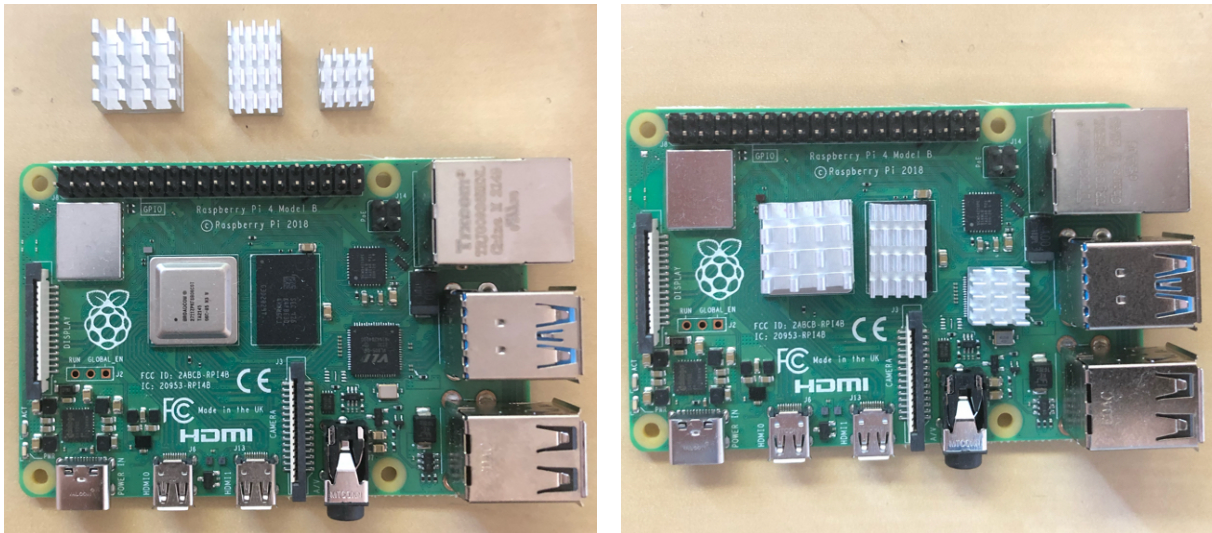


Figure 4: Raspberry PI 4; left: without installed heat sinks; right: with installed heat sinks; in addition a fan for cooling was installed inside the housing (not shown in this figure).

2 Three-axis magnetometer

For the measurement of the terrestrial magnetic field the following system will be used. The main electronic components are the Raspberry Pi 4 Model B from okdo Technology and three FLC100 magnetic field sensors from Stefan Mayer Instruments GmbH & Co. KG. To connect these components a differential 8 channel 18 bit Analog to Digital Converter (ADC) from AB Electronics UK was used. The digital temperature sensor TMP102 from Sparkfun Electronics was installed to monitor the temperature near the magnetic field sensors.

2.1 Raspberry PI 4

To prepare the hardware setup of the Raspberry PI 4, the *okdo Company's guide*¹ was followed. The heat sinks (see Fig. 4), the fan for cooling and then the SD card were installed. The interfaces were connected: keyboard, mouse, monitor and the power plug. Then the Raspberry PI was switched on and the installation instructions on the screen were followed.

In order to make sure that latest OS Version and software packages are installed the *instruction guideline* from Raspberry PI² was followed. For initial Python programming tests the already installed integrated development environment *Thonny Python IDE* was used.

2.2 Analog Digital Converter

For the installation and setup of the 8 channel 18 bit ADC from AB Electronics UK the analog outputs of the FLC100 magnetic sensors (OUT+ and OUT-) were connected to the ADC. The converter has two MCP3424 (each 4 channels) microchips onboard, which can be controlled via an Inter-Integrated Circuit (I2C) bus interface³ and converts the analog sensor input

¹Okdo, *Get started with your okdo Pi kit in a Flash!*, <https://www.okdo.com/getstarted/>

²Raspberry Pi Documentation, <https://www.raspberrypi.com/documentation/computers/os.html>

³Microchip Technology, *18-Bit, Multi-Channel Analog-to-Digital Converter with I2CTM Interface and On-Board Reference*, <https://www.robotshop.com/media/files/content/a/abu/pdf/mcp3424.pdf>

voltage to a digital value. The I2C bus interface is used for the communication between the Raspberry PI and the other circuit parts. It is based on the master-slave principle, which means that the data transfer is initiated by the master (Raspberry PI). The slaves (connected components) have their own unique addresses and respond to the request from the master. The data is transferred via the data line (SDA). The serial clock runs on the second signal line (SCL) and is used to transmit the bus clock from the master. The Raspberry PI then reads a digital value from the series of incoming bits.

For the system setup, the following pins must be connected between the Raspberry PI and the ADC:

- Power +5.0 V
- Power +3.3 V
- GND
- I2C bus lines SDA and SCL

Once the power and I2C interface has been set up, it can be tested from the terminal command line:

```
i2cdetect -y 1
```

The response to this command confirms that a I2C device with addresses 68 and 69 is available at the I2C bus, which are the two ADC converts on the ADC board:

```
user@raspberrypi:~ $ i2cdetect -y 1
    0  1  2  3  4  5  6  7  8  9  a  b  c  d  e  f
00:          -- -- -- -- -- -- -- -- -- -- -- -- -- --
10: -- -- -- -- -- -- -- -- -- -- -- -- -- -- --
20: -- -- -- -- -- -- -- -- -- -- -- -- -- -- --
30: -- -- -- -- -- -- -- -- -- -- -- -- -- -- --
40: -- -- -- -- -- -- -- -- -- -- -- -- -- -- --
50: -- -- -- -- -- -- -- -- -- -- -- -- -- -- --
60: -- -- -- -- -- -- -- -- 68 69 -- -- -- -- -- --
70: -- -- -- -- -- -- -- -- --
```

Six out of eight channels of the ADC are used, where each magnetic sensor (for the three dimensions) has two output voltages. With the 18 bits, one used for the information, whether the value is negative or positive, one gets a precision of 17 bits⁴, which means 15.625 μ V.

To control the ADC and read the analog sensor values, the software library *ADCPi* was used⁵.

To validate the output voltage of the ADC via the I2C bus, the 3.3 V on-board voltage was applied to all eight channels of the ADC. Since this value can deviate, it was additionally checked via a multimeter. The Raspberry PI then read out the voltage values from the ADC via the I2C bus lines. The Python script used for this can be found in appendix 6. It was noticed that the output voltage values of the eight channels did not match the input voltage displayed on the multimeter. As a potential root cause the tolerance of the voltage dividers

⁴Microchip Technology, *18-Bit, Multi-Channel Analog-to-Digital Converter with I2CTM Interface and On-Board Reference*, <https://www.robotshop.com/media/files/content/a/abu/pdf/mcp3424.pdf>

⁵AB Electronics, *AB Electronics UK ADC Pi Python Library*, https://github.com/abelectronicsuk/ABElectronics_Python_Libraries/tree/master/ADCPi

Table 1: Results of a calibration measurement for the eight ADC channels with the reference voltage $U_{\text{ref}} = 4.070 \text{ V}$.

ADC channel	Measured voltage [V]	Calibration parameter
1	4.078	0.998
2	4.069	1.000
3	4.059	1.003
4	4.073	0.999
5	4.071	1.000
6	4.076	0.999
7	4.076	0.999
8	4.069	1.000

(resistors) on the ADC board was assumed. To determine this difference more accurately, the same measurement was performed again with a 3.7 V LiPo battery. The calibration parameters in Table 1 have been identified and will be used for all further measurements. The reference voltage supplied by the battery was $U_{\text{ref}} = 4.070 \text{ V}$.

2.3 Magnetic field sensor FLC100

The used magnetic field sensors FLC100 from Stefan Mayer Instruments GmbH & Co. KG⁶ are high-resolution flux gate sensors for weak magnetic fields (see Fig. 5). The following pins must be connected to the ADC:

- Power +5.0 V
- GND
- OUT+
- OUT-

The flux gate principle is used for sensors with high sensitivity. The sensor consists of a ferromagnetic core surrounded by a coil. A current flow in the coil magnetizes the core. Without an external magnetic field, a symmetrical voltage curve would be generated in the coil. If there is indeed an external magnetic field, an asymmetry is measured, which can be read off from the output voltages OUT+ and OUT-.

The FLC100 needs a +5 V power supply and has a 2 mA current consumption. The output voltage is proportional to the magnetic flux density and the measuring range is $\pm 100 \mu\text{T}$. The maximum output voltage (OUT+ against OUT-) is $\pm 2.5 \text{ V}$, where 1 V represents $50 \mu\text{T}$. The measurement accuracy at 20°C is $\pm 2\%$, which means $\pm 0.3 \mu\text{T}$. In order to track the robustness and the variance of the sensors, a short Python script was used for testing. It is shown in appendix 6.

The results of this measurement can be seen in Fig. 6. After some time of stabilization, the variance of the magnetic field is below 10 nT. When entering the room, the light was switched on and the mobile phone was activated. This was done by intent in order to see the effect from other devices (see last peak). One sees that it is very important to choose an environment with as least interfering sources as possible.

⁶Stefan Mayer Instruments, *Magnetfeldsensor FLC 100*, https://stefan-mayer.com/images/datenblaetter/Datenblatt_FLC-100.pdf

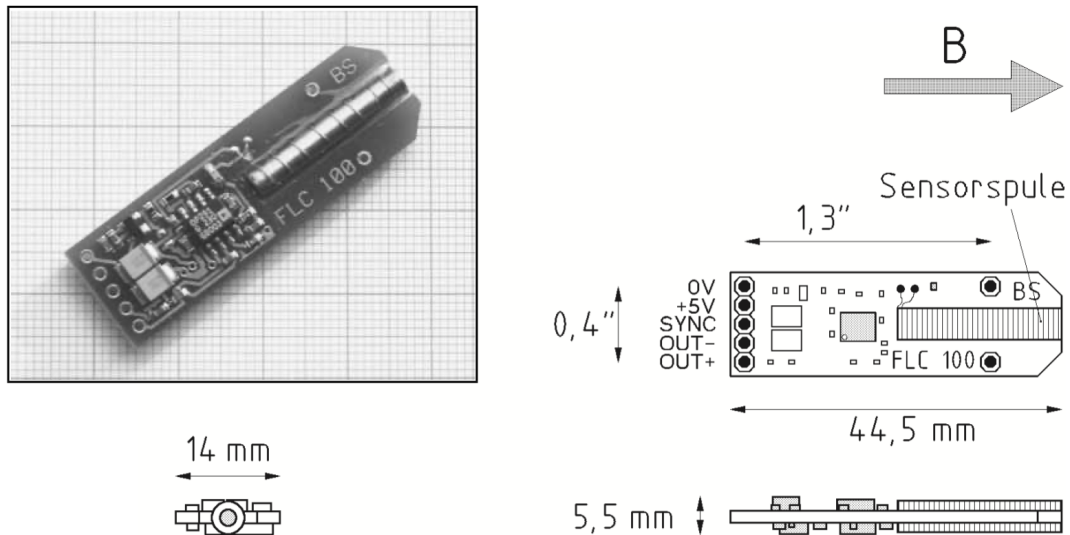


Figure 5: The FLC100 with the five pins (0V, +5V, SYNC, OUT+, OUT-); image taken from Stefan Mayer Instruments⁷

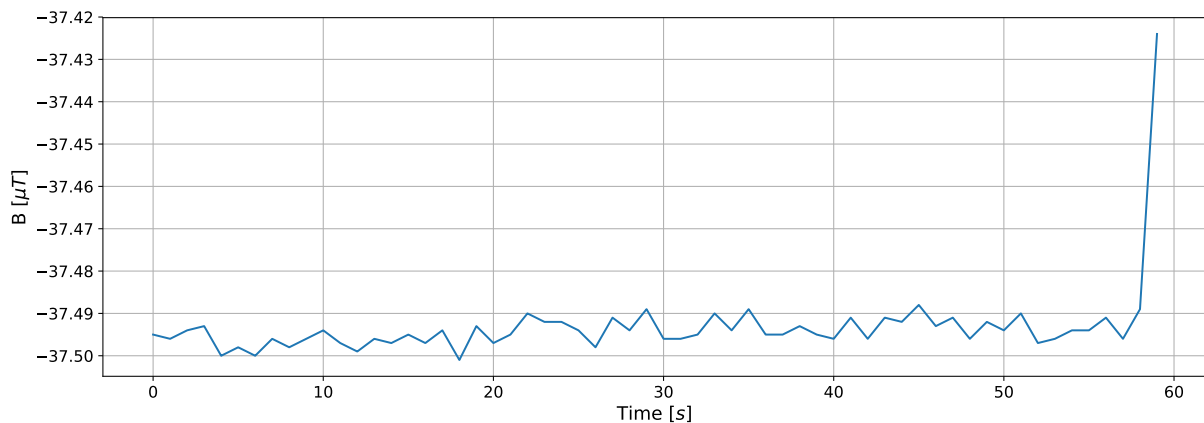


Figure 6: Results of a test measurement of the magnetic field in one direction parallel to the earth's surface. The peak in the last 5 seconds is caused by entering the room, switching on the light and by mobile phone activity.

The initial magnetic field testing was done with jumper wires between the system components. There should be even less noise, once the system is assembled on the breadboard with soldered copper wires.

2.4 Temperature sensor TMP102

For measuring the temperature near the magnetic sensors the digital temperature sensor TMP102 from Sparkfun Electronics⁸ was selected. It has an I2C interface to provide its data to the Raspberry Pi on request.

⁷Stefan Mayer Instruments, *Magnetfeldsensor FLC 100*, https://stefan-mayer.com/images/datenblaetter/Datenblatt_FLC-100.pdf

⁸Melopero, <https://www.melopero.com/shop/sensori/temperatura/sparkfundigitaltemperaturesensorbreakouttmp102/>

The following pins need to be connected between the Raspberry PI and the temperature sensor:

- Power +3.3 V
- GND
- I2C bus lines SDA and SCL

The I2C search function was used again to verify the correct interconnection of the temperature sensor.

```
user@raspberrypi:~ $ i2cdetect -y 1
    0  1  2  3  4  5  6  7  8  9  a  b  c  d  e  f
00:                -- -- -- -- -- -- -- -- -- -- -- -- -- --
10: -- -- -- -- -- -- -- -- -- -- -- -- -- -- -- --
20: -- -- -- -- -- -- -- -- -- -- -- -- -- -- -- --
30: -- -- -- -- -- -- -- -- -- -- -- -- -- -- -- --
40: -- -- -- -- -- -- -- -- 48 -- -- -- -- -- -- -- --
50: -- -- -- -- -- -- -- -- -- -- -- -- -- -- -- --
60: -- -- -- -- -- -- -- -- 68 69 -- -- -- -- -- -- --
70: -- -- -- -- -- -- -- -- --
```

An additional I2C device with address 0x48 appears, which can be assigned to the temperature sensor. A Python library for the TMP102 from Sparkfun was used to install and test the sensor⁹. To check the function I wrote a short Python script, which can be seen in appendix 6.

The room temperature was printed as the following:

```
Current temp: 24.8°C
```

A thermometer measured the current room temperature with the result of 24.8°C and validated the printed temperature of the TMP102 sensor.

⁹Github, *Python Library for reading temperature data from the TMP102 breakout board from Sparkfun*, <https://github.com/n8many/TMP102py>

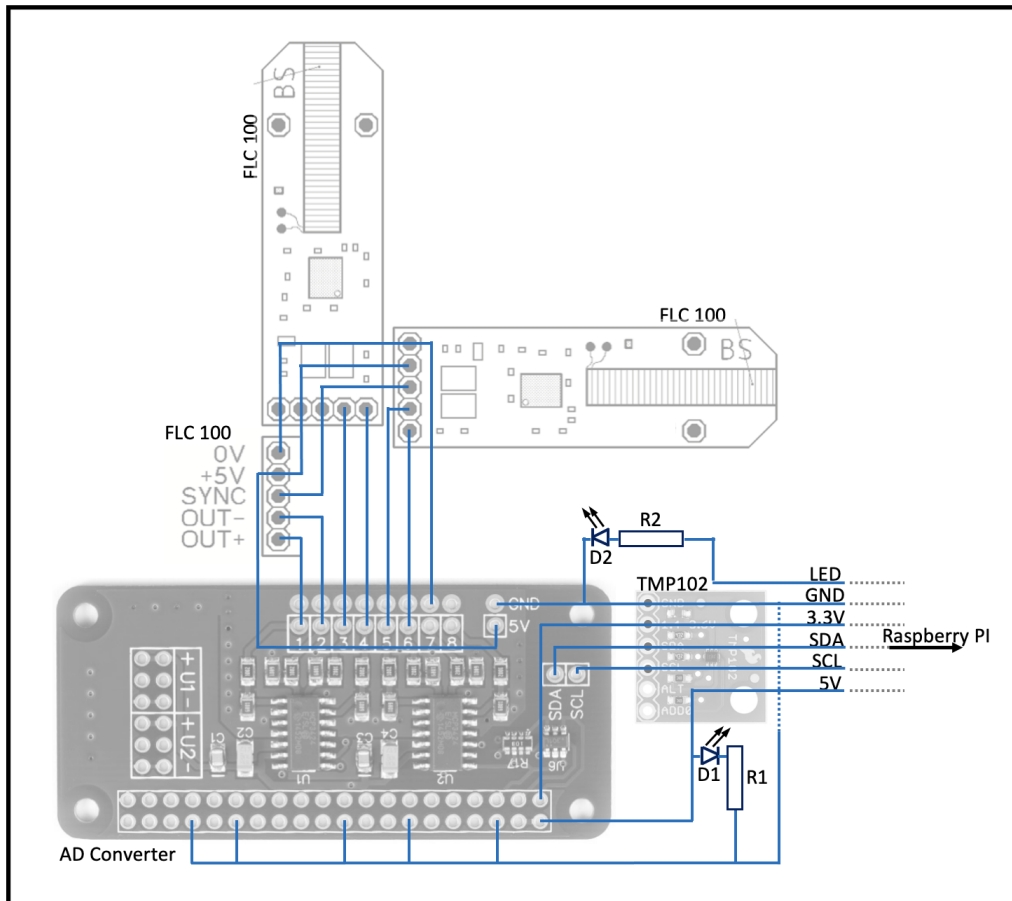


Figure 7: Wiring diagram of all components, exclusive of the Raspberry PI; the three FLC100 magnetic field sensors¹⁰ are connected to the AD Converter¹¹. The ADC and the TMP102 temperature sensor¹² use the same I2C bus lines, which are connected to the Raspberry PI.

2.5 Wiring diagram

All components were soldered to a breadboard with a wire strand. Fig. 7 shows the wiring diagram to build a complete magnetometer (without the Raspberry PI).

The FLC100 magnetic sensors are interconnected with the 0V, +5V and SYNC terminals. 0V and +5V are also connected to the ADC. In addition, the OUT+ and OUT- outputs of the three magnetic sensors are each connected to the ADC, which converts the analog signal to a digital value that can be passed to the Raspberry PI.

The ground lines of all components are connected. The SDA and SCL signal lines from the Raspberry PI are connected to the ADC and the TMP102. Since the temperature sensor already outputs a digital value on the I2C bus, its data does not need to be converted by the ADC. The voltages of +3.3V and +5V needed by the ADC are also supplied by the Raspberry PI.

Furthermore there are two LEDs D1 and D2 with two resistors R1 and R2 on the board. D1 lights up permanently as soon as the system is connected to the power supply to indicate a

¹⁰https://stefan-mayer.com/images/datenblaetter/Datenblatt_FLC-100.pdf

¹¹<https://www.abelectronics.co.uk/docs/stock/raspberrypi/adcpizero/adcpizero-3.jpg>

¹²Melopero, <https://www.melopero.com/shop/sensori/temperatura/sparkfundigitaltemperaturesensorbreakouttmp102/>

Table 2: Configuration of the three FLC100 magnetic field sensors with OUT+ and OUT- connected to the ADC.

ADC channel	Magnetic sensor output
1	Z OUT+
2	Z OUT-
3	Y OUT-
4	Y OUT+
5	X OUT-
6	X OUT+
7	not used
8	not used

working system. D2 is connected to the Raspberry PI via a signal line and can be controlled. It was used during test runs to indicate individual measurements by toggling. During the actual measurement it was not switched on and off to avoid a disturbing magnetic field. Table 2 shows the configuration of the FLC100 sensors connected to the ADC.

3 Analysis software

After bringing all components together, I wrote a Python script to read out the temperature and magnetic field data.

To minimize outliers, several values are combined into an average in the code. The numbers of samples are stored in the values `adc_samples` and `temperature_samples`. Then a timer was implemented to get out of the room before the measurement starts. It was set to 120 sec. The main loop consists of a part that is meant to read the magnetic sensor values and then calculate an average of 50 values. Through this step we obtain 1 minute data, which are stored in the list `ADC_AVG`. Because problems with reading the I2C values occurred during test runs, a try and except query was added to prevent the program from hanging. If such an error comes up, after a pause of 2 sec the measurement of the next values is continued. The calculated values of the temperature sensor and the three magnetic sensors are written to a csv file together with the current date and time. One has to be careful not to override existing files by executing the code again. The final code can be found in appendix 6.

4 Measurements

Two measurements were started under similar but not identical conditions. Both were performed at the Dr. Karl Remeis-Observatory in Bamberg. An unused room at 7–8 m depth was chosen to have as few sources of interference as possible. There are no electronic devices and no power cables except the one that supplies the measuring device. The nearest main road is about 100 m away. At this depth the temperature is quite stable, which makes the measurement easier and more accurate. Because of these conditions, this basement room was chosen for the measurement. The second measurement was started because unforeseen results appeared in the first measurement, which should be investigated by another measurement. The results are discussed in chapter 4.1 and 4.2.

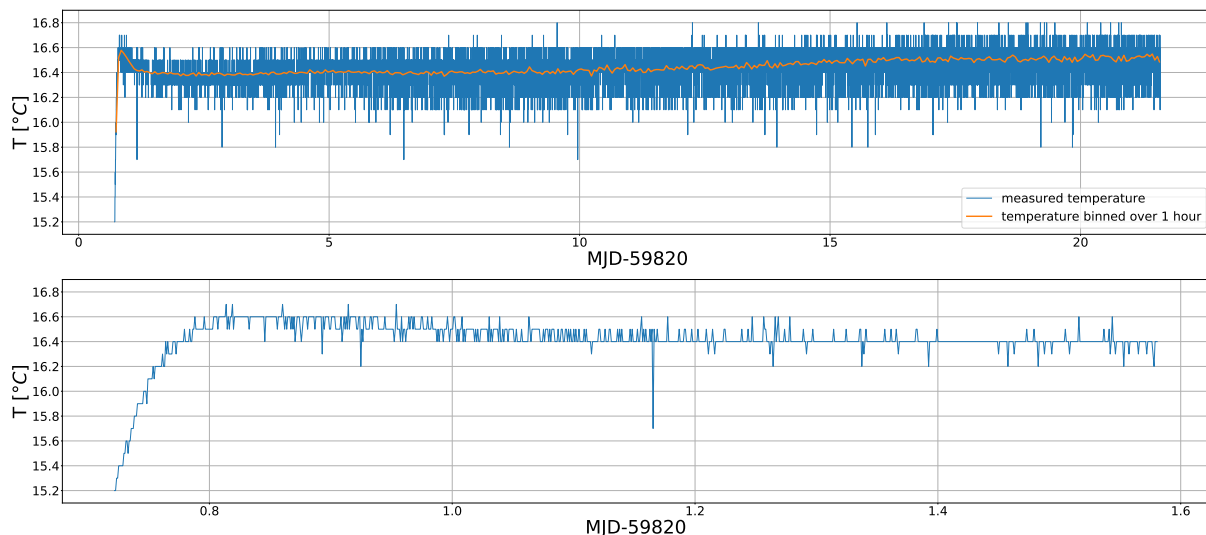


Figure 8: Top: total temperature results of the first measurement, blue: measured values, orange: values binned over 1 h; bottom: zoom on the first 1000 temperature values with an increase from 15.2°C to 16.6°C within 61 minutes; time is given in Modified Julian Date-59820

4.1 First three weeks measurement

With the described setup a three weeks long measurement was done between 29 August 2022 and 19 September 2022. Simultaneously, the temperature and the magnetic values in x -, y - and z -direction were measured. The entire setup was located in an isolated and waterproof box with a size of approximately $40 \times 60 \times 15 \text{ cm}^3$. The z -axis of the magnetometer pointed in zenith. x and y were rotated around the z -axis, so that the x -value took the largest possible value and therefore pointed parallel to the local magnetic field. To set the magnetic field sensors up that way, the script was running on a monitor and the sensors were moved until the x -value reached a maximum. Afterwards the measurement was started without the monitor.

4.1.1 Temperature

Fig. 8 shows the measured temperature values plotted over time given in Modified Julian Date (MJD)-59820. The MJD is a continuous count of years, starting at midnight on 17 November 1858. It was noticeable that within 61 minutes the setup heats up from 15.2°C to 16.6°C and then settles at $16.4 \pm 0.1^\circ\text{C}$.

This increase was expected, because the whole system was in one isolated box. The heat of the Raspberry PI influences the FLC100 magnetic sensors and therefore the measured magnetic field. In a second measurement this was changed. This will be discussed in chapter 4.2.

The increasing temperature shows that it makes sense to observe only the magnetic field values after the warm-up phase in the first 61 minutes. After this time the temperature stays nearly stable.

Temperature analysis using a histogram showed a roughly Gaussian distribution with an upward trend. Therefore, the values were binned over time intervals of 1 h. This reduces the noise of the temperature sensor and the increase in temperature becomes more visible (see Fig. 8).

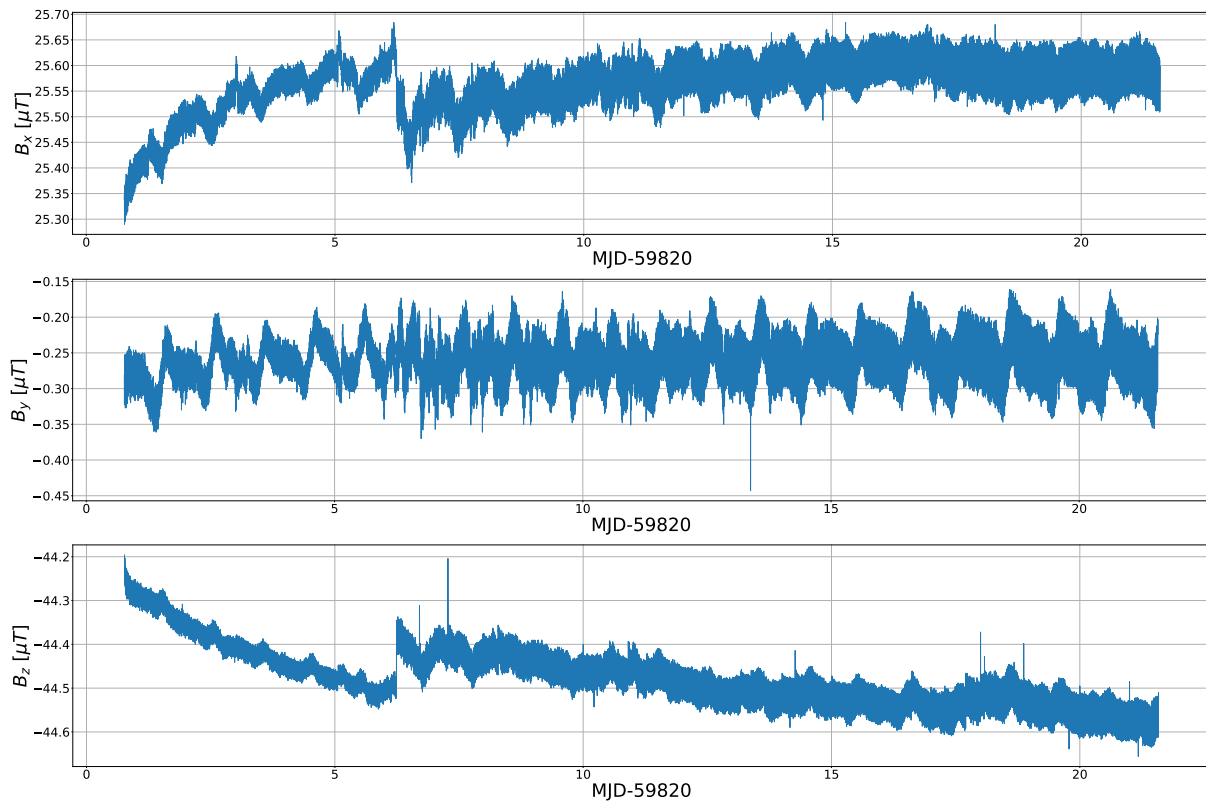


Figure 9: Total magnetic sensor results in x -, y - and z -dimension of the first measurement; at $\text{MJD}-59820 = 6.543$ a kink occurs in all three dimensions, but can be seen especially in x - and z -direction

4.1.2 Magnetic field values in the three dimensions

After cutting the data from the first 61 minutes the remaining results of the magnetic field in three dimensions can be seen in Fig. 9. Some conspicuous features were immediately noticeable:

- In x - and y -direction, the value of the magnetic field increases over the entire measurement period.
- In the z -direction, this value decreases over the entire measurement.
- Periodicities can be seen in all directions, which are at least roughly in the range of 24 h.
- At $\text{MJD}-59820 = 6.543$ a kink is visible in all three dimensions, but can be seen especially in x - and z -direction, which also changes the following measurement results permanently.

Periodicities of approximately 24 h and 9 min are recognizable. These were examined in more detail with the help of epoch folding, a method of timing analysis. Therefore the program is given the assumption of a period value, which then 'folds' the data over exactly this period. If there is no periodicity in this time period, high and low values average out and a constant value is obtained. If there is indeed a periodicity, the maxima add up and a peak becomes visible. With this method the following periods were determined in all three

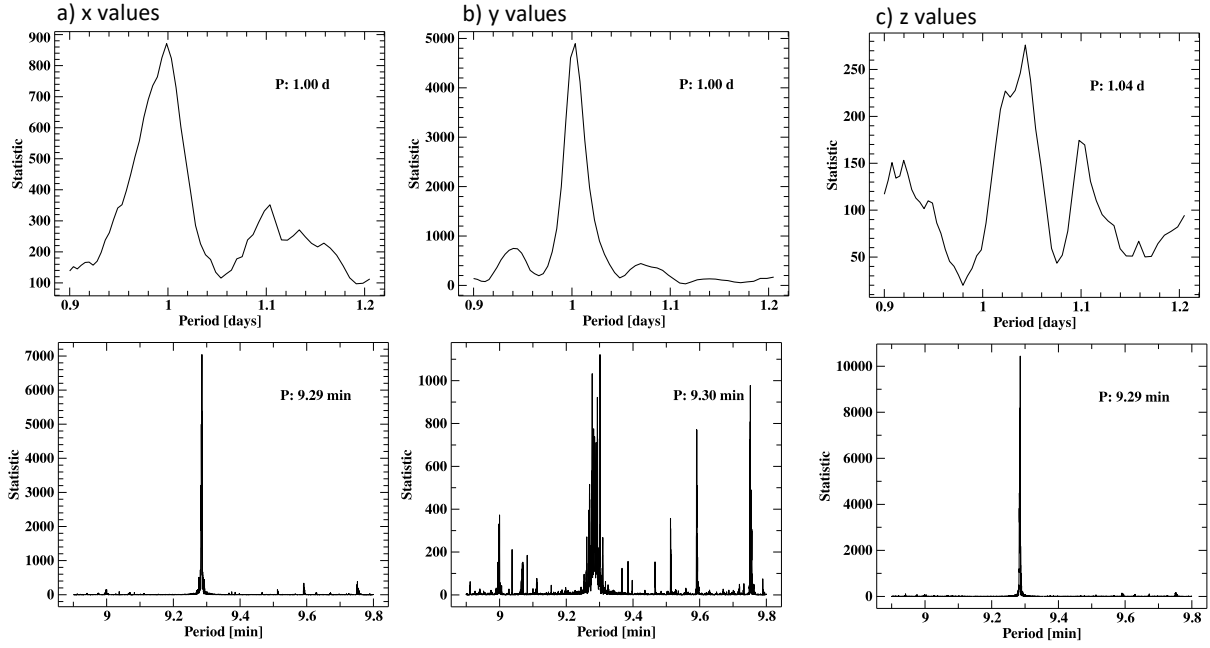


Figure 10: Results of the epoch folding to find periodicities in the magnetic field values in all three dimensions of the first measurement; a) x -values; b) y -values; c) z -values

dimensions (see Fig. 10):

$$\begin{aligned}
 P_{1,x}^1 &= 1.00 \text{ d} & P_{1,x}^2 &= 9.29 \text{ min} \\
 P_{1,y}^1 &= 1.00 \text{ d} & P_{1,y}^2 &= 9.30 \text{ min} \\
 P_{1,z}^1 &= 1.04 \text{ d} & P_{1,z}^2 &= 9.29 \text{ min}
 \end{aligned}$$

4.1.3 Total magnetic field values

Particularly interesting is also the absolute value of the total magnetic field because it is more comparable to other magnetic data

$$B_{\text{tot}} = \sqrt{B_x^2 + B_y^2 + B_z^2}. \quad (1)$$

The values were calculated for the first measurement and are shown in Fig. 11. The kink at $\text{MJD}-59820 = 6.543$ and the known periods can be found again. In Fig. 11 one plot is zoomed to five 24 h periods and another one is zoomed to several 9 min periods. Occurring periods were also investigated by epoch folding for the total values of the magnetic field. Since this method is hindered by the kink at $\text{MJD}-59820 = 6.543$, the period after the kink alone was also examined. Both results are shown in Fig. 12. The periods found are

$$\begin{aligned}
 P_{1,\text{tot}}^1 &= 1.02 \text{ d} & P_{1,\text{tot}}^2 &= 9.29 \text{ min} \\
 P_{1,\text{cut}}^1 &= 1.02 \text{ d} & P_{1,\text{cut}}^2 &= 9.29 \text{ min.}
 \end{aligned}$$

According to the epoch folding plots in Fig. 12 the calculation for the area after the kink makes much more sense for the 1.02 d periodicity than the one over the entire measurement,

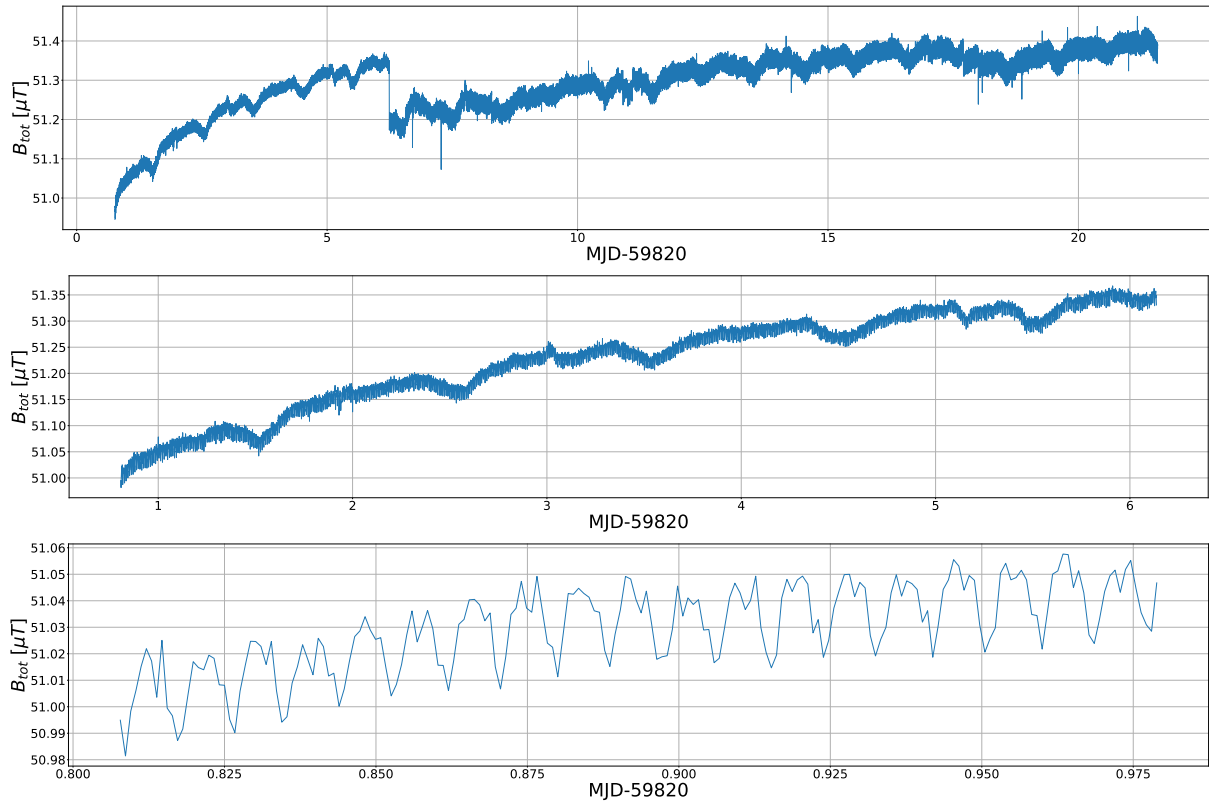


Figure 11: Total magnetic field values of the first measurement; top: whole measurement period; middle: zoom on five 24 h periods; bottom: zoom on 9 min periodicity

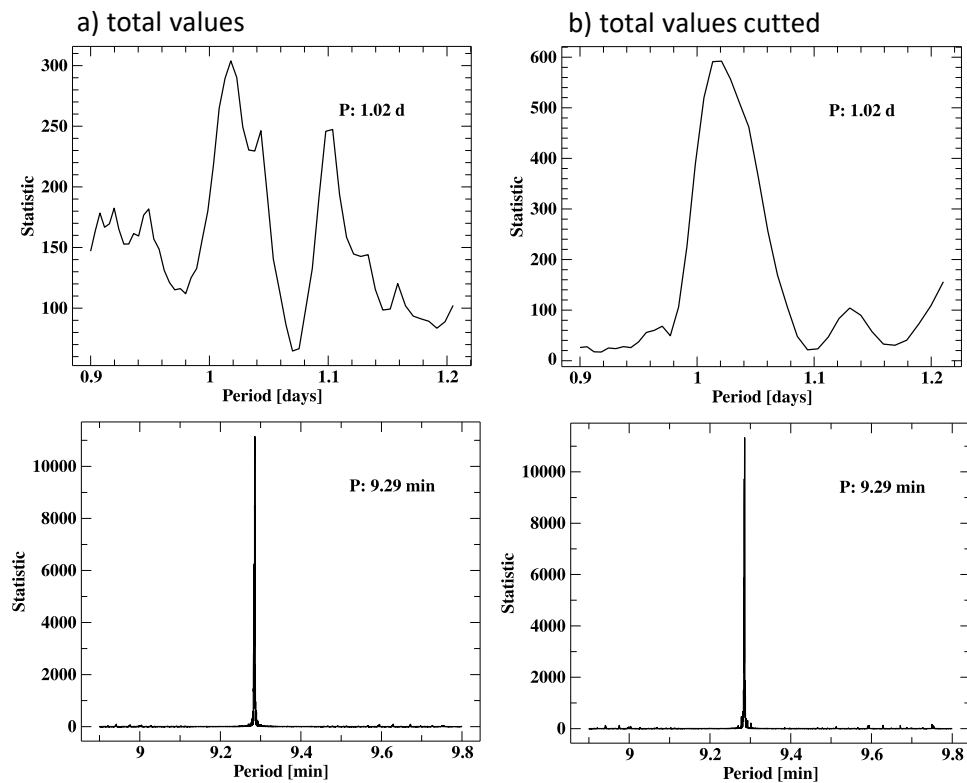


Figure 12: Results of the epoch folding to find periodicities in the total magnetic values of the first measurement

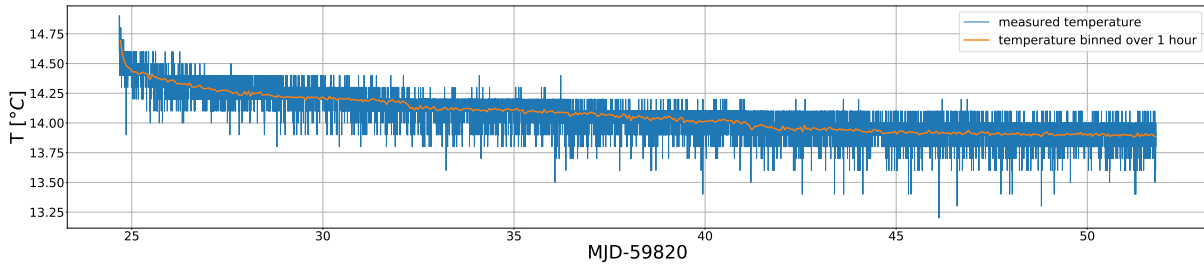


Figure 13: Total temperature results of the second measurement; a rapid cooling in the first 4.596 h occurs; then a decrease in temperature is noticeable over the entire measurement period, this is due to the beginning of autumn and the resulting drop in outside temperatures.

even though it shows the same value for the period. For the 9.29 min period both results are very sharp and similar.

To better understand the cause of the periodicities and the kink at $\text{MJD}-59820 = 6.543$, another measurement was started under similar conditions.

4.2 Second four weeks measurement

Using the same technical setup, a new measurement was done for four weeks from 22 September 2022 to 19 October 2022. The z -axis of the magnetometer still pointed vertical. Directions of x and y were again aligned so that the x -value took the largest possible value.

The difference to the first measurement was that the Raspberry PI was in its own isolated and waterproof box, and thus could no longer influence the temperature sensor and the FLC100 magnetic sensors.

4.2.1 Temperature

In contrast to the first measurement, where the entire setup initially warmed up due to the heat from the Raspberry PI, the temperature sensor records a drop in temperature for 4.596 h at the beginning (see Fig. 13). This is because it was still stored at outside temperature (approximately 19°C) a few minutes before the measurement started. Then it was moved to the same cool basement room as used for the first measurement (approximately 14°C). A cooling of the environment can be seen over the entire measuring period. This is due to the dropping temperature values between 22 September 2022 and 19 October 2022. A roughly Gaussian distribution of the temperature values was also found in Fig. 13, as in the first measurement. The values were binned over 1 h to average over the noise of the temperature sensor.

4.2.2 Magnetic field values in the three dimensions

The x - and y -values in Fig. 14 show an increase over the measurement period, while the z -values decrease over this time. This could also be observed in the first measurement. But in contrast to the first measurement, no kink in the measured values can be seen here.

Again, periods of about 24 h and 9 min are visible. The epoch folding gives the following

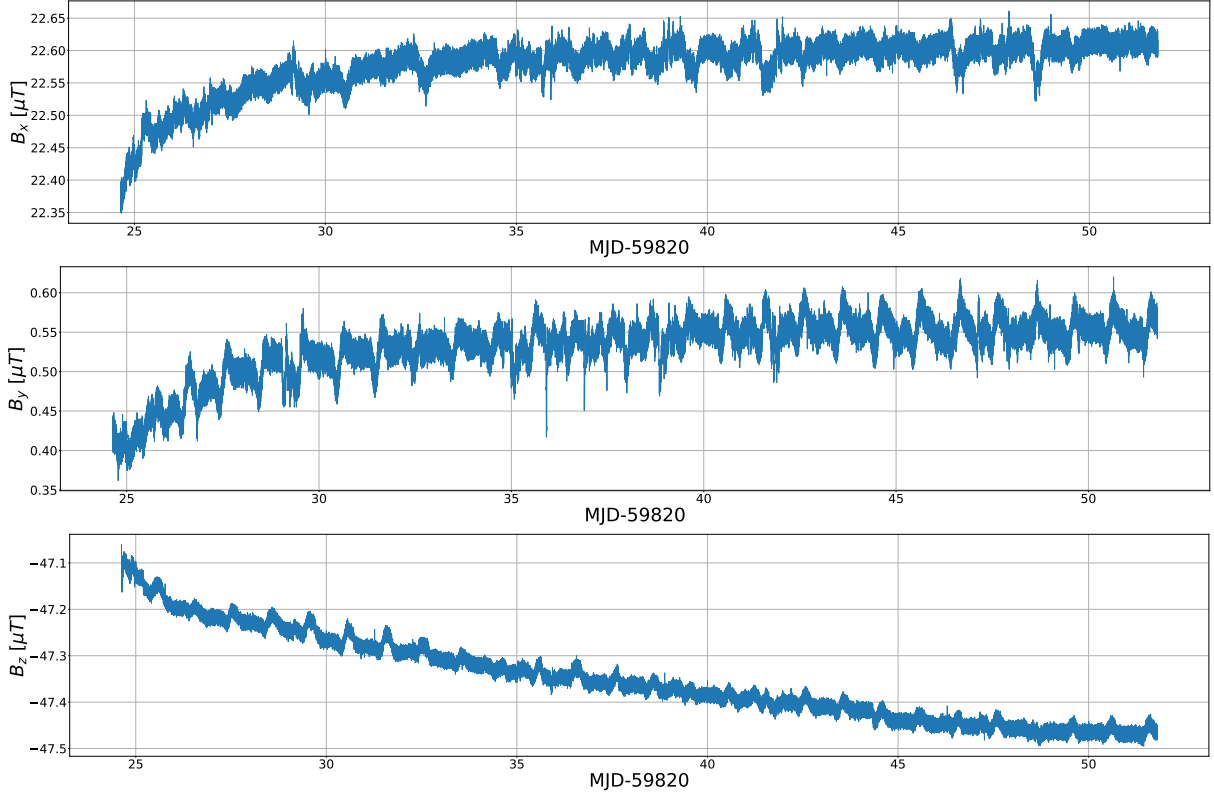


Figure 14: Magnetic sensor results in x -, y - and z -dimension of the second measurement.

results (see Fig. 15):

$$\begin{aligned}
 P_{2,x}^1 &= 1.00 \text{ d} & P_{2,x}^2 &= 9.28 \text{ min} \\
 P_{2,y}^1 &= 1.00 \text{ d} & P_{2,y}^2 &= 9.28 \text{ min} \\
 P_{2,z}^1 &= 1.00 \text{ d} & P_{2,z}^2 &= 9.28 \text{ min}
 \end{aligned}$$

The found periods in all three dimensions matched with a precision of two decimal places.

4.2.3 Total magnetic field values

All dimensions combined to the total magnetic field B_{tot} (1) are shown in Fig. 16. The values increase over the time, and again the known periods are visible, which are verified via epoch folding analysis in Fig. 17.

$$P_{\text{tot}}^1 = 1.00 \text{ d} \qquad P_{\text{tot}}^2 = 9.28 \text{ min}$$

These were expected based on the results of the individual magnetic field values and their periods. There is a general increase, which is stronger at the beginning and then decreases over time.

5 Temporal variation of the magnetic field

To better assess the functionality of the built magnetometer, the measured data will be examined in more detail in this chapter and compared to data from other observatories.

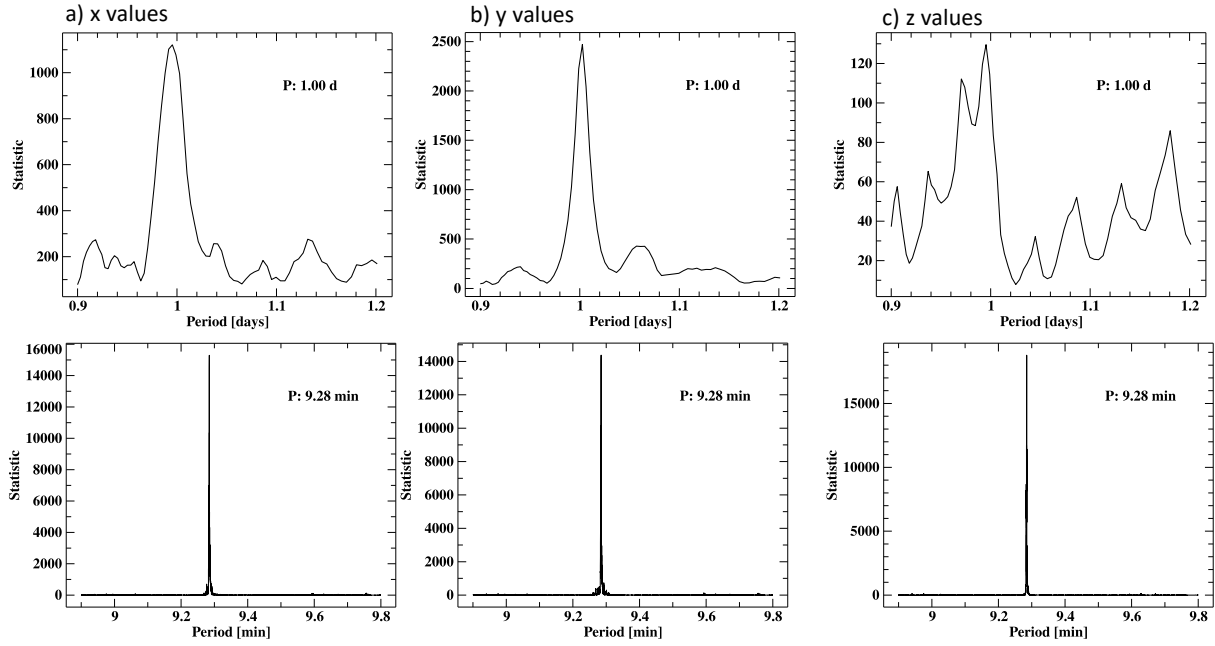


Figure 15: Results of the epoch folding analysis from the magnetic field values in each direction of the second measurement.

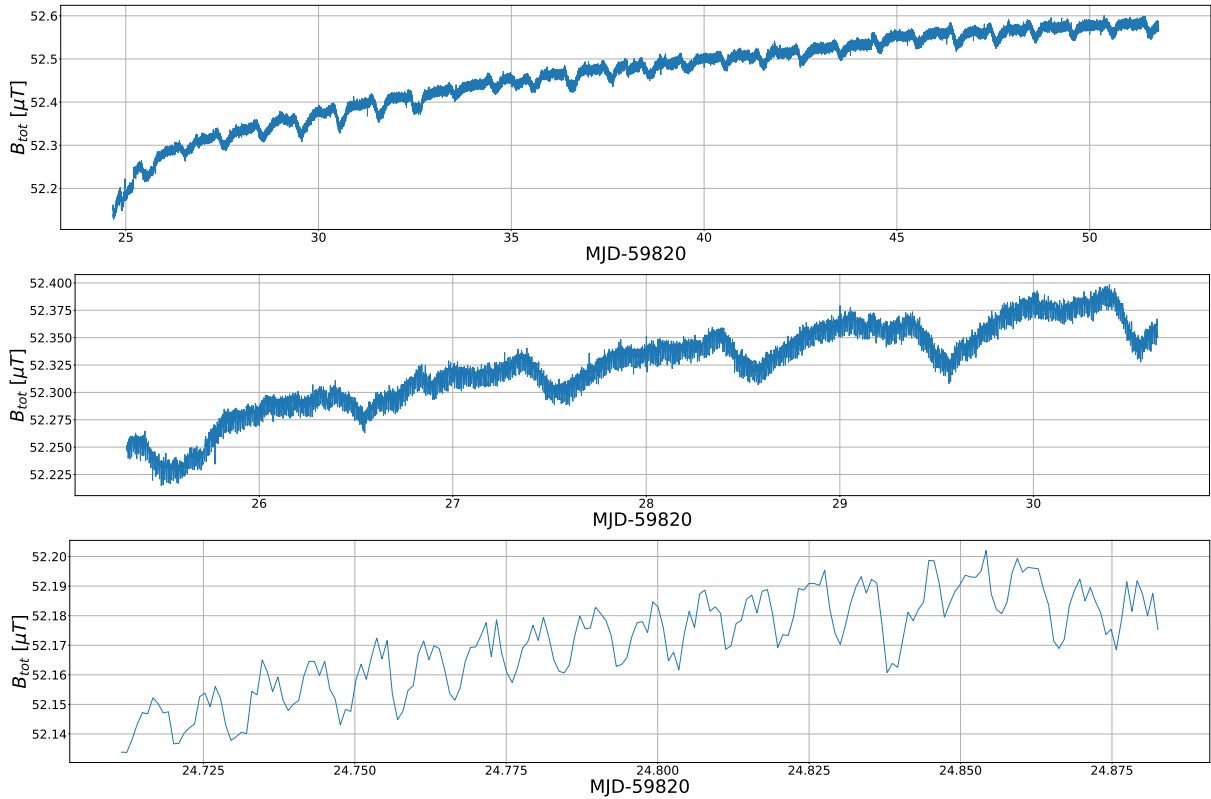


Figure 16: Total magnetic field values of the second measurement; top: whole measurement period; middle: zoom on five 24 h periods; bottom: zoom on 9 min periodicity.

The general rises and falls in the data and the possible causes of the two periodicities are discussed.

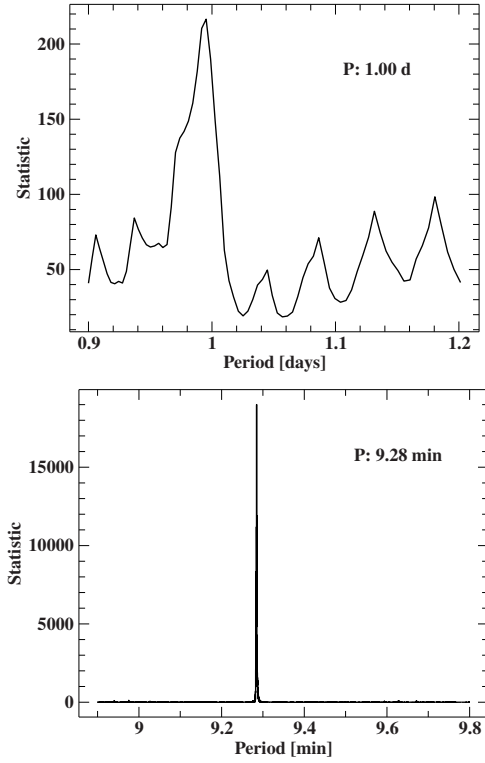


Figure 17: Results of the epoch folding analysis from the total magnetic field values of the second measurement.

5.1 General in/decreases

Both measurements show increases and decreases in the magnetic field. In addition, the measured values are on average about 3400 nT higher than comparable values from the Geophysical Observatory Fürstfeldbruck. According to Michal Vlk from the observatory Budkov, this can be caused by strong magnetic objects. Since the measurements at the Dr. Karl Remeis-Observatory were carried out underground, but directly under the observatory and the dome building, this is a good explanation for generally too high values. In addition, no calibration of the magnetic sensors was performed at a known and constant magnetic field. So it is possible that there is an offset in the data and the sensors show a value different to zero, even if the magnetic field value is actually $B_{\text{tot}} = 0$ T. To better compare the trends in the data, the continuous offset was subtracted and the data average was set to $B_{\text{tot}} = 0$ T.

To verify the measured data, comparative data from the Adolf Schmidt Observatory for Geomagnetism in Niemegek (NGK) were used. These were chosen because of their geographical location close to Bamberg. They are 1 minute data of all three dimensions, converted to a total magnetic field using equation (1). These data are publicly available and accessible via the International Real-time Magnetic Observatory Network¹³ (INTERMAGNET), a global network of observatories monitoring the earth's magnetic field.

Because of the difference in longitude $d_{\text{BAM-NGK}}$ between Bamberg and Niemegek, the data must be adjusted in time. The comparative data from Niemegek are adjusted by

$$t = \frac{d_{\text{BAM-NGK}} \cdot 24 \text{ h}}{2\pi r_{\oplus}} = 0.08394 \text{ h.} \quad (2)$$

¹³Intermagnet, <https://intermagnet.github.io>

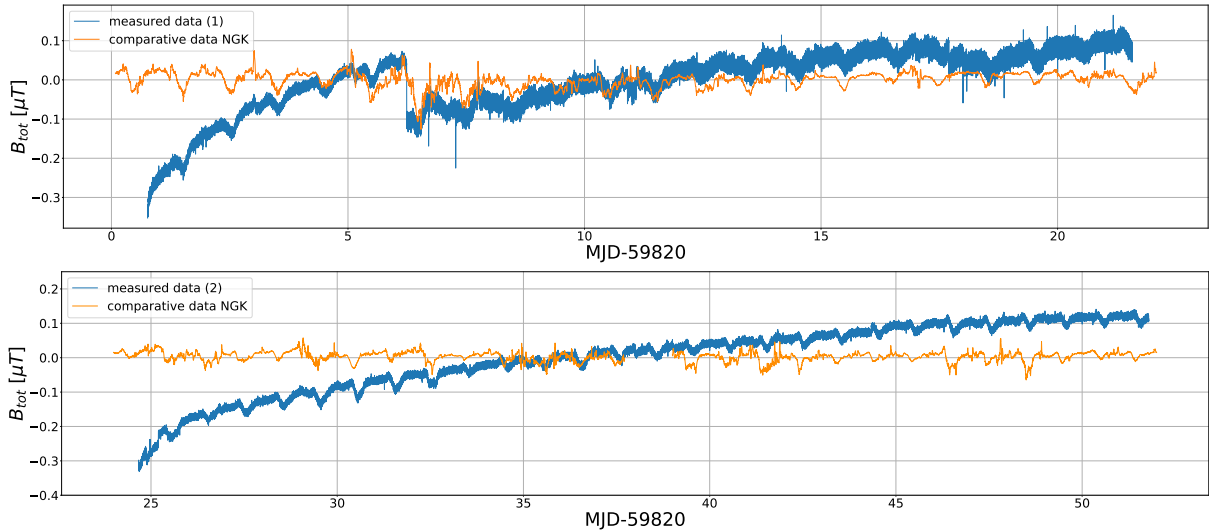


Figure 18: Comparison of the measured data in Bamberg and the magnetic field data from Niemegek¹⁴ (NGK); top: first measurement from 29 August 2022 to 19 September 2022; bottom: second measurement from 22 September 2022 to 19 October 2022.

For the comparison data in the second measurement period, there was a problem with the data recording between $\text{MJD}-59820 = 37.7932$ and $\text{MJD}-59820 = 39.0779$ and default values of $3.4028 \cdot 10^{38}$ nT were entered, which of course do not allow any meaningful interpretation. They were therefore removed from the comparison data.

In the measured data of the total magnetic field from Bamberg, increases are visible. If one compares the results with comparative data in Fig. 18, it can be seen that these cannot be caused by the earth's magnetic field.

The first assumption of a cause was a spatial slippage of the board during the experiment, which could shift the magnetic field in the individual dimensions. But since the total magnetic field also increases, this can be excluded. It is interesting that an increase can be seen in the total magnetic field strengths of both measurements.

The magnetic field sensors are temperature dependent, but temperature variation as the main cause for these variations can be ruled out by the fact that in the first measurement, after a period of settling, the temperature was approximately constant, but an increase in the total magnetic field was still visible. Furthermore, a temperature difference does not explain why the z -values decrease while the x - and y -values increase.

It is very likely that over the time of the measurement, some parts of the setup have become statically charged. No grounding was present during the measurements. With such accurate data, this can lead to increases as visible in Fig. 18.

In a conversation with Rudolf Widmer-Schmidrig from the Black Forest Observatory, the seismologist confirmed that general upward and downward drifts are a big issue in geomagnetics.

5.2 9.29 min periodicity

In order to better compare the periodicities, the measured data from Bamberg were polynomially fitted and this increase was then calculated out. For the fit of the first measurement

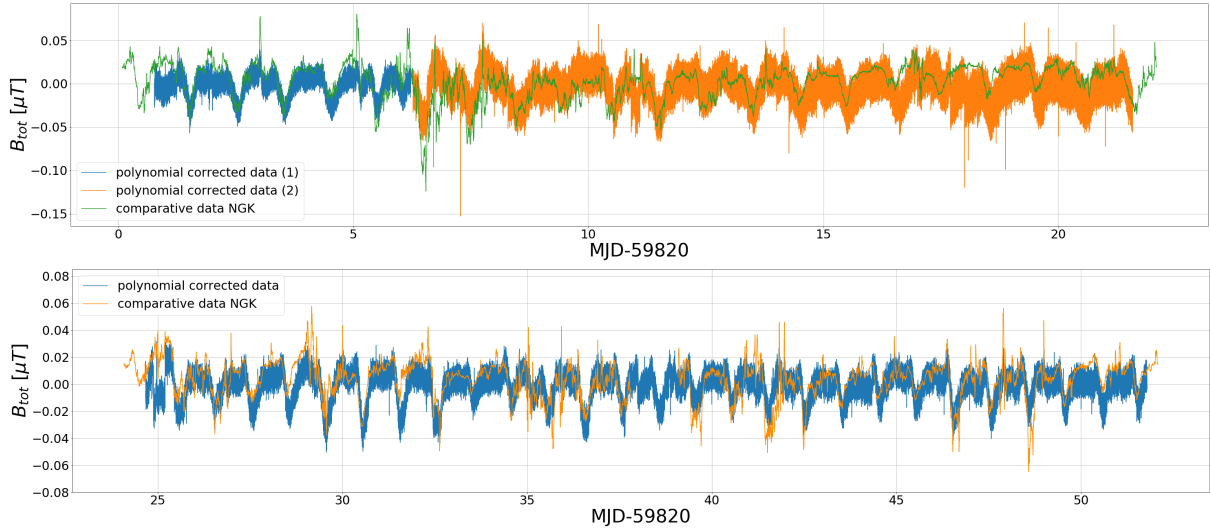


Figure 19: Comparison of the measured data in Bamberg (polynomial corrected), and the magnetic field data from Niemegek¹⁵ (NGK); top: first measurement, divided in two parts before and after the kink; bottom: second measurement.

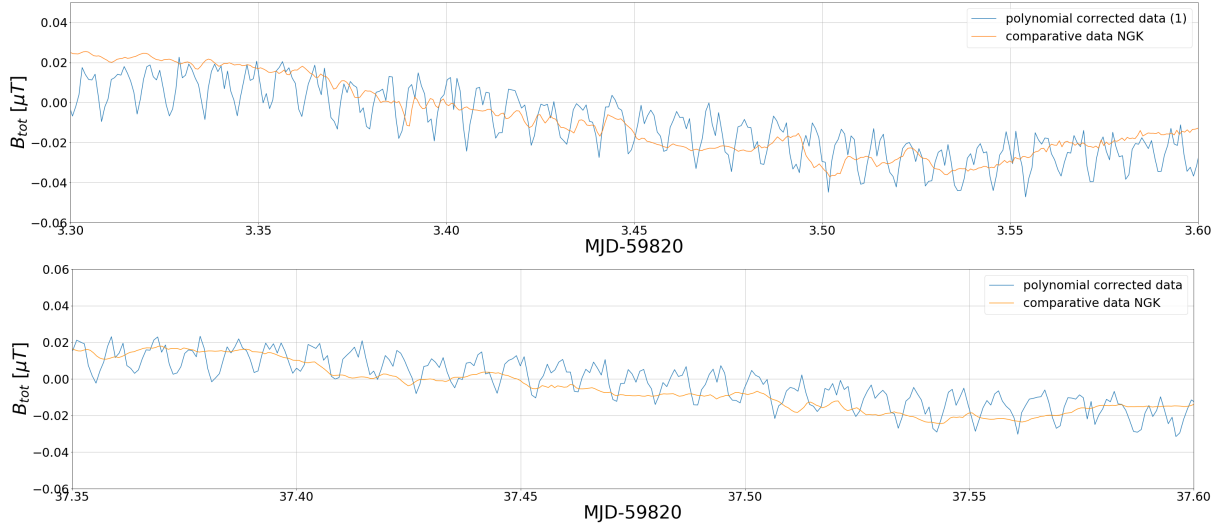


Figure 20: Comparison of the measured data in Bamberg (polynomial corrected), and the magnetic field data from Niemegek (NGK); top: first measurement; bottom: second measurement; zoom on 9 min periodicity in both plots.

the data were divided into two parts. One before the kink and one after to be able to fit more precisely. Afterwards only the periodicities and individual deflections can be seen, but no longer the general upward trends. The results can be seen in Fig. 19.

The data from Bamberg have an apparently stronger noise in Fig. 19. In a smaller time range (see Fig. 20) the 9 min periodicities become visible. These periodicities were also visible in the analysis via epoch folding (see chapter 4.1 and 4.2).

¹⁴Intermagnet, <https://intermagnet.github.io>

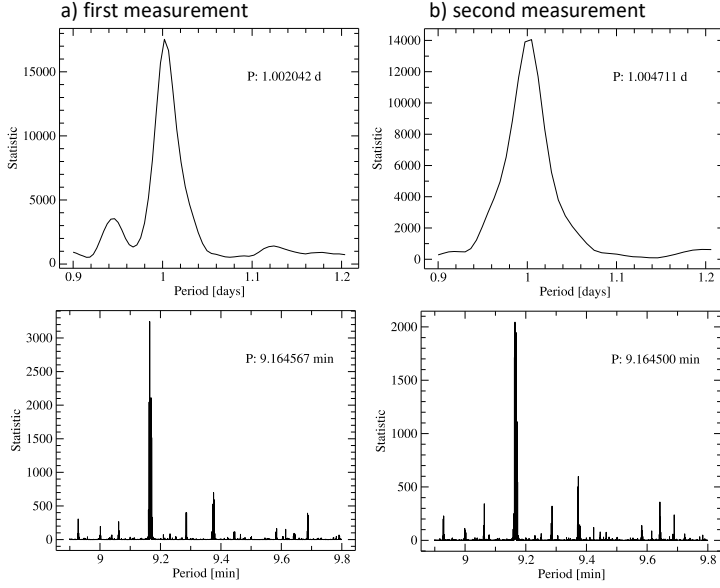


Figure 21: Results of the epoch folding analysis to find periodicities in the total magnetic field values of the data from Niemegek; a) comparative data for the period from 29 August 2022 to 19 September 2022; b) comparative data for the period from 22 September 2022 to 19 October 2022.

When analyzing the comparative data from Niemegek, similar results were noticed:

$$P_{1,\text{tot}}^2 = 9.29 \text{ min}$$

$$P_{2,\text{tot}}^2 = 9.28 \text{ min}$$

$$P_{1,\text{NGK}}^2 = 9.16 \text{ min}$$

$$P_{2,\text{NGK}}^2 = 9.16 \text{ min}$$

A natural origin of these periods can be excluded, since no cause with a frequency of 1.794 mHz (Bamberg) or 1.820 mHz (Niemegek) is known. The first approach was the comparison with local mobile phone frequencies, but these are at significantly higher values in the MHz range and can therefore be excluded. An actual origin could be a device with an electric motor, for example an air conditioner. It cannot be excluded that the 9 min periods come from this.

5.3 24 h periodicity

To better compare the daily periodic variations, the measured data from Bamberg were binned over 9.29 min. Thus these periods are no longer visible and single events and the 24 h periods can be analyzed better. The binned data got plotted for both measurements in Fig. 22. In the first measurement at $\text{MJD} - 59820 = 6.543$ the comparative data from Niemegek also show a downward kink (see Fig. 19). This seems to be not only an effect of the measuring technique in Bamberg, but an actual event in the earth's magnetic field.

The markers in Fig. 22 indicate times where other deflections are visible in both data sets. The magnetometer built in Bamberg can therefore not only record the daily periodic fluctuations quite accurately, but also make events in the earth's magnetic field visible.

Comparing the values of the period analysis via epoch folding from chapter 4.1 and 4.2 with the determined periods of the comparison values from Niemegek (see Fig. 21), it shows a

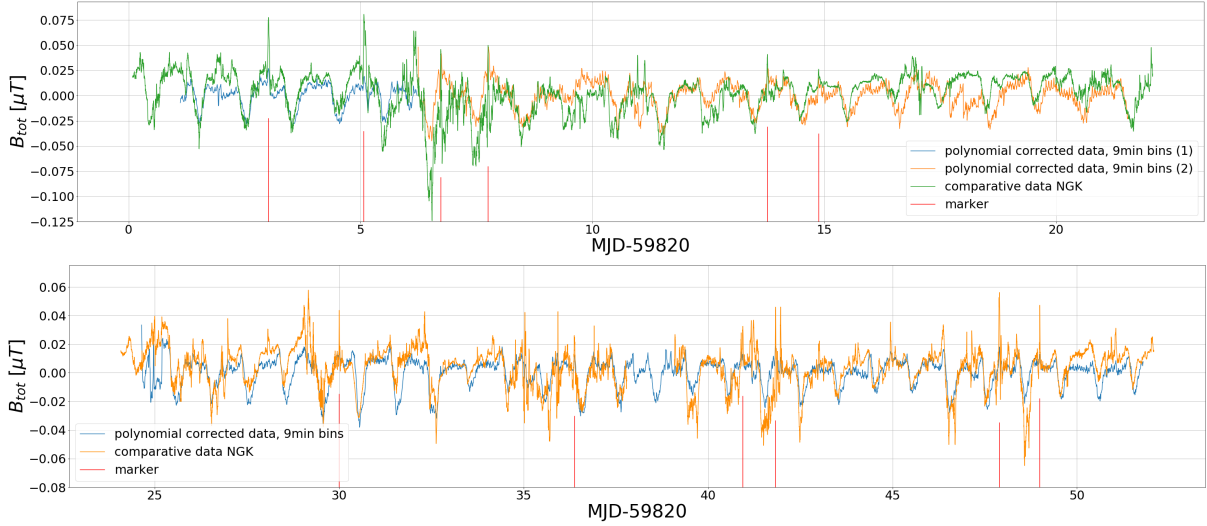


Figure 22: Comparison of the measured data in Bamberg (polynomial corrected and binned over 9.29 min) and magnetic field data from Niemegek¹⁶(NGK); top: first measurement; bottom: second measurement; the markers show events that can be seen in both sets of data

high agreement.

$$P_{1,\text{tot}}^1 = 1.02 \text{ d}$$

$$P_{2,\text{tot}}^1 = 1.00 \text{ d}$$

$$P_{1,\text{NGK}}^1 = 1.00 \text{ d}$$

$$P_{2,\text{NGK}}^1 = 1.00 \text{ d}$$

With an accuracy of two decimal places $P_{2,\text{NGK}}^1$ and $P_{2,\text{tot}}^1$ agree exactly. Between $P_{1,\text{tot}}^1$ and $P_{1,\text{NGK}}^1$ there is a deviation of 2%.

These periods actually find their origin in the geomagnetic field. When solar radiation hits the earth's atmosphere, it heats up. The differential solar radiation is also called solar tides. In the upper region of the ionosphere, the ionospheric dynamo layer is found. It is characterized by an electrically conducting plasma which is moved by the solar tides. The movement against the geomagnetic field lines induces electric currents and thus also a magnetic field, as in a dynamo. These variations are called Sq (solar quiet) variations (Schubert, 2007).

The lines in Fig. 23 indicate the direction of the magnetic field, while the density of the lines is proportional to the height-integrated current density (Schubert, 2007). As the earth rotates, an observatory passes under these ring currents. If it is located on the northern hemisphere of the earth (just like Bamberg and Niemegek), the field lines point from south to north in the morning, and from north to south in the evening. These fluctuations create the daily periods in the magnetic field measurements in Bamberg and Niemegek.

At the geomagnetic equator, the effects of the ring currents are less visible. From the southern hemisphere the effects are recognizable, although they are reversed. At night, there is a quiet phase in these currents (Schubert, 2007).

¹⁵Intermagnet, <https://intermagnet.github.io>

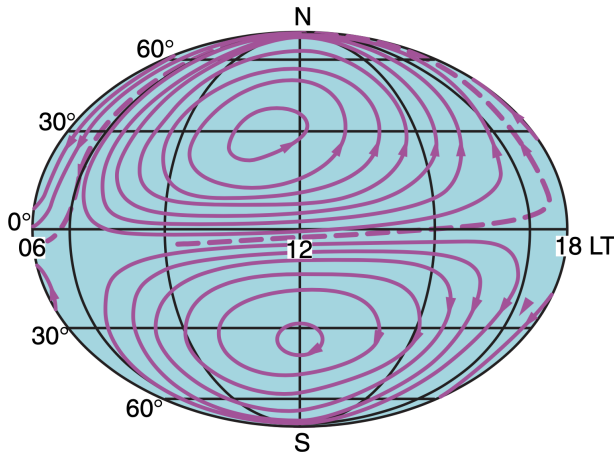


Figure 23: Dayside view of the Sq current system (image taken from Schubert, 2007, their Fig. 9 in chapter 3).

6 Conclusions

The aim of this thesis was to measure and analyze the earth's magnetic field and its daily variations with a Raspberry PI based magnetometer. This was successful and with the help of comparative data from the Adolf Schmidt Observatory for Geomagnetism in Niemeck the measured data could be validated. Thereby the 24 h periods, caused by ring current systems on the northern hemisphere, matched very well.

The two major weaknesses in the data were an increase in total magnetic field values over the measurement period of the measurements and a general offset, presumably caused by strong magnetic objects or a wrong calibration of the sensors.

To better understand these two deviations from comparative data, further test measurements over longer periods of time are needed. This would allow us to determine if the average of the measured values is constant after a long period of time, as we might suspect. To exclude static charging of the components, the system should be grounded and the Raspberry PI should be shielded (Faraday cage). Possibly, this will eliminate the increases in the data, which are similar to the charging curve of a capacitor.

Stuart Gilder from the Department of Earth and Environmental Sciences at the Ludwig Maximilian University Munich recommended a measurement with an oscilloscope at the same socket that was used for the magnetic field measurements. With a timing analysis it should then become clear whether the 9 min period can originate from the network. Stefan Mayer, manufacturer of the FLC100 magnetic sensors, recommended an exclusively battery-powered measurement after seeing the magnetic field data from Bamberg. This should be done in order to exclude interfering effects from the power network.

For the 9 min periods found, there is no clear answer what they are. But it can be assumed that they come from an electric motor located near the measuring device. To exclude these periods it would be useful to perform the measurements at another location. The Black Forest Observatory uses a mine for their measurements, which leads 200 m into the mountain, as can be seen in Fig. 24. There, the temperature is very stable and there are no sources of interference in the surroundings (Widmer-Schnidrig et al., 2018). A new measurement at this location in cooperation with Rudolf Widmer-Schnidrig from the Black Forest Observatory is a reasonable next step.

Once these issues are resolved, magnetic data measured on the earth's surface should be compared with satellite data to infer how solar radiation and particles interact with the

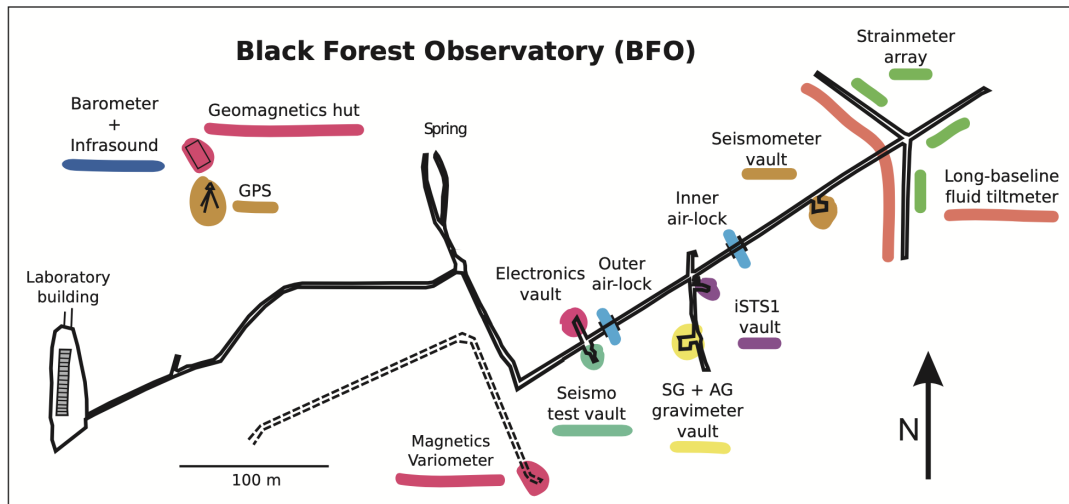


Figure 24: Anton Mine underground system from the Black Forest Observatory. At the end of a 200 m long tunnel (dashed lines) there are magnetic variometers. In a deeper, 700 m long corridor further measuring stations are installed (image taken from Widmer-Schmidrig et al., 2018, their Fig. 2.1).

earth's atmosphere. Understanding how much solar storms can affect magnetic fields, the next step is to investigate how much damage the triggered variations in the magnetic field and the high-energy particles themselves could cause in modern technology if a major outburst towards earth occurs.

References

- Beggan C.D., Marple S.R., 2016, *Astron. Geophys.* 57, 2.24
- Dmitriev A.V., Huang C.M., Brahmanandam P.S., et al., 2013, *J. Geophys. Res. (Space Physics)* 118, 6806
- Loi S.T., Murphy T., Cairns I.H., et al., 2015, *Geophys. Res. Lett.* 42, 3707
- Matsumoto Y., Miyoshi Y., 2022, *Geophys. Res. Lett.* 49, e2022GL101037
- Owocki S., 2022, plenary review for IAUS 370 in press (arXiv:2210.17472)
- Ponti G., Sanders J.S., Locatelli N., et al., 2022, *Astron. Astrophys.* in press (arXiv:2211.02060)
- Reda R., Giovannelli L., Alberti T., 2022, *Adv. Space Res.* in press (arXiv:2210.07855)
- Schubert G., 2007, *Treatise on geophysics*, Vol. 5, Elsevier, Amsterdam
- Widmer-Schnidrig R., Duffner P., Forbriger T., Zürn W., 2018, In: Heck A. (ed.) (Schw)Ehre, wem (Schw)Ehre gebührt: Festschrift zur Verabschiedung von Prof. Dr.-Ing. Dr. h.c. Bernhard Heck, Vol. 1. Schriftenreihe des Studiengangs Geodäsie und Geoinformatik, KIT Scientific Publishing, Karlsruhe, p.281

Appendix

Python script for validating the ADC

```

from ADCPi import ADCPi
import time
#===== ADC and I2C Bus Setup =====
adc = ADCPi(0x68, 0x69, 18)
#===== Main Loop for Testing =====
adc.set_pga(1) #Set the gain of the PGA on the chip
adc.set_bit_rate(18) # Set the sample bit rate of the adc
adc.set_conversion_mode(0) #Set the One-shot conversion mode

while True:
    print('{:>5.5f} '.format(adc.read_voltage(1)) +
          '{:>5.5f} '.format(adc.read_voltage(2)) +
          '{:>5.5f} '.format(adc.read_voltage(3)) +
          '{:>5.5f} '.format(adc.read_voltage(4)) +
          '{:>5.5f} '.format(adc.read_voltage(5)) +
          '{:>5.5f} '.format(adc.read_voltage(6)) +
          '{:>5.5f} '.format(adc.read_voltage(7)) +
          '{:>5.5f} '.format(adc.read_voltage(8)))
    time.sleep(0.3)

```

Python script for validating the FLC100

```

#External calibration voltage from Multimeter (Battery)
ExtCalVoltage = 4.0705
Calibration = [4.078, 4.0689, 4.059, 4.073, 4.071,
4.076, 4.076, 4.069] #Calibration parameters per channel
for c in range(8):
    Calibration[c] = ExtCalVoltage/Calibration[c]

#===== ADC and I2C Bus Setup =====
adc = ADCPi(0x68, 0x69, 18)
adc_samples = 20 # Number of samples, used for mean value
adc.set_pga(1) #Set the gain of the PGA on the chip
adc.set_bit_rate(18) # Set the sample bit rate of the adc
adc.set_conversion_mode(1) #Set the Continuous conversion

#===== Main Loop for Testing =====
while True:
    ADC_AVG = list()
    for c in range(2): # Read the first 2 Channels (Out+ and Out-)
        ADC_Input = list()
        for i in range(adc_samples): # Take samples
            ADC_Input.append(adc.read_voltage(c+1)*Calibration[c])

```

```

ADC_AVG.append((sum(ADC_Input))/adc_samples) # Get average

#Calculate and print magnetic field (units are  $\mu$ T)
MagneticSensorValue = (ADC_AVG[0]-ADC_AVG[1])*50
print('{:>1.3f}'.format(MagneticSensorValue))

#Write data to .csv
now = datetime.datetime.now() # Get System Time
file = open(csvFile, "a")
file.write(now.strftime('%H:%M:%S') + Del +
'{:>1.3f}'.format(MagneticSensorValue).replace('.',',') + '\n')
file.close()

```

Python script for validating the TMP102

```

import time
from tmp102 import TMP102

# Initialize TMP102 Object
temperature = TMP102(units='C', address=0x48, busnum=1)

while True:
    print ('Current temp: {:.1f}°C'.format(temperature.readTemperature()))
    time.sleep(1)

```

Complete Python script

```

#=====
# Import Libraries
#=====
import time
from ADCPi import ADCPi
import datetime
from gpiozero import LED
from TMP102_Lib import TMP102

#=====
# Initialize TMP102 Object (Temperature Sensor)
#=====
Temperature_Sensor = TMP102(units='C', address=0x48, busnum=1)
temperature_samples = 10 # Number of samples, used for mean value

#=====
# CSV File Setup
#=====
Del = ';' #csv delimiter

```

```

csvHeader = 'Day' + Del + 'Month' + Del + 'Year' + Del + 'Time' + Del
+ 'Temperature(°C)' + Del + 'X-Value(µT)' + Del + 'Y-Value(µT)' + Del
+ 'Z-Value(µT)' + '\n'
csvFile = "/home/user/results.csv"
# setup new csv file (!!! overrides existing file !!!)
file = open(csvFile, "w")
file.write(csvHeader)
file.close()

#=====
# ADC and I2C Bus Setup
#=====
adc = ADCPi(0x68, 0x69, 18)
adc_samples = 50 # Number of samples, used for mean value
adc.set_pga(1) #Set the gain of the PGA on the chip
adc.set_bit_rate(18) # Set the sample bit rate of the adc
adc.set_conversion_mode(1) #Set conversion mode for the adc to One-shot

#=====
# ADC Calibration Data (compensate tolerances of ADC Voltage Divider)
#=====
ExtCalVoltage = 4.0705 #External calibration voltage
Calibration = [4.078, 4.0689, 4.059, 4.073, 4.071,
4.076, 4.076, 4.069] #Calibration parameters per channel
for c in range(8):
    Calibration[c] = ExtCalVoltage/Calibration[c] #use calibration values

#=====
# Leave the Room Timer
#=====
print("120 sec left")
time.sleep(120) # timer for 120 sec

#-----
#===== Main Loop =====
#-----
while True:
    I2C_exception = False
    #=====
    # READ MAGNETIC SENSOR VALUES
    #=====
    ADC_AVG = list()
    for c in range(6): # Read all magnetic se5nsor values (Channel 1-6)
        ADC_Input = list()
        for i in range(adc_samples): # Take n Samples
            try:
                ADC_Input.append(adc.read_voltage(c+1)*Calibration[c])

```

```

        except IOError as e:
            now = datetime.datetime.now() # Get System Time
            print(now.strftime('%H:%M:%S'), "I2C exception occurred")
            time.sleep(2)
            I2C_exception = True
    ADC_AVG.append((sum(ADC_Input))/adc_samples) # Get average

#=====
# Calculate Magnetic Fields
#=====
#calculate magnetic field (units are  $\mu$ T): OUT+ minus OUT-
MagneticSensorValue_Z = (ADC_AVG[0]-ADC_AVG[1])*50
MagneticSensorValue_Y = (ADC_AVG[3]-ADC_AVG[2])*50
MagneticSensorValue_X = (ADC_AVG[5]-ADC_AVG[4])*50

#=====
# READ TEMPERATURE
#=====
Temperature_AVG = list()
for i in range(temperature_samples): # Take m samples
    try:
        Temperature_AVG.append(Temperature_Sensor.readTemperature())

    except IOError as e2:
        now = datetime.datetime.now() # Get System Time
        print(now.strftime('%H:%M:%S'), "Temperature exception occurred")
        time.sleep(2)
        I2C_exception = True

Temperature = (sum(Temperature_AVG)/temperature_samples) # Get average

#=====
# WRITE DATA TO FILE
#=====
if not I2C_exception:
    file = open(csvFile, "a")
    now = datetime.datetime.now() # Get System Time
    file.write(now.strftime('%d') + Del)
    file.write(now.strftime('%m') + Del)
    file.write(now.strftime('%Y') + Del)
    file.write(now.strftime('%H:%M:%S') + Del)
    file.write('{:.1f}'.format(Temperature).replace('.',',')+Del)
    file.write('{:.3f}'.format(MagneticSensorValue_X).replace('.',',')+Del)
    file.write('{:.3f}'.format(MagneticSensorValue_Y).replace('.',',')+Del)
    file.write('{:.3f}'.format(MagneticSensorValue_Z).replace('.',',')+'\n')
    file.close()

```

Danksagung

Zunächst möchte ich mich bei meinem Betreuer Prof. Dr. Jörn Wilms bedanken, der mich nicht nur in dieser Arbeit unterstützt hat, sondern mir auch schon ganz früh in meinem Studium das Tor zur Astronomie geöffnet hat. Danke Jörn, für Deine Hilfe in allen Fragestellungen und danke, dass Du meine chaotischen Ideen in eine gute Reihenfolge gebracht hast.

Außerdem möchte ich Philipp Thalhammer und Ole König danken. Ihr habt mich bei der Auswertung der Daten immer wieder unterstützt. Ohne Eure Hilfe wäre ich an einigen Tagen deutlich ratloser an meinem Arbeitsplatz gesessen.

Ein besonderer Dank geht auch an Dr. Rudolf Widmer-Schnidrig vom Geowissenschaftlichen Gemeinschaftsobservatorium (BFO). Danke, dass Du dir mehrmals die Zeit genommen hast, mit mir über meine Ergebnisse zu diskutieren.

Des Weiteren bedanke ich mich bei Dipl.-Phys. Dr. Stefan Mayer, der mir immer bei meinen Fragen zu den Magnetsensoren weiterhelfen konnte.

Vielen Dank auch an Prof. Dr. Stuart Gilder vom Department für Geo- und Umweltwissenschaften in München und Dipl. Ing. Michal Vlk, Ph.D. vom Observatorium Budkov, die mich ebenfalls bei der Interpretation der Daten unterstützt haben.

Zuletzt möchte ich mich bei meinem Vater Jürgen Grabmann bedanken. Du hast mir nicht nur von klein auf das Interesse an Naturwissenschaften mitgegeben, sondern auch während dieser Arbeit immer wieder mit mir über die Problemstellungen diskutiert. Vielen Dank für die angeborene Leidenschaft zur Physik.

Erklärung

Hiermit versichere ich, dass ich die vorliegende Arbeit selbstständig verfasst und keine anderen als die angegebenen Quellen und Hilfsmittel benutzt habe, dass alle Stellen der Arbeit, die wörtlich oder sinngemäß aus anderen Quellen übernommen wurden, als solche kenntlich gemacht sind und dass die Arbeit in gleicher oder ähnlicher Form noch keiner Prüfungsbehörde vorgelegt wurde.

Erlangen, den 15.11.2022